Trumbull, R. B., Yang, J.-S., Robinson, P. T., di Pierro, S., Vennemann, T., Wiedenbeck, M. (2009): The carbon isotope composition of natural SiC (moissanite) from the Earth´s mantle. New discoveries from ophiolites. - Lithos, 113, 3-4, 612-620

DOI: 10.1016/j.lithos.2009.06.033

The carbon isotope composition of natural SiC (moissanite) from the Earth's mantle: new discoveries from ophiolites

Robert B. Trumbull[1], Jing-Sui Yang[2], Paul T. Robinson[1], Simonpietro Di Pierro[3], Torsten Vennemann[4], Michael Wiedenbeck[2]

[1]GFZ German Research Centre for Geosciences, Telegrafenberg, Potsdam, 14473 Germany

[2] Key Laboratory for Continental Dynamics, Institute of Geology, Chinese Academy of Sciences, Beijing, 100037 China

[3] Applied Mineralogy Group, Saint-Gobain Recherche, Aubervilliers Cedex, F-93303 France

[4]Institute of Mineralogy and Geochemistry, University of Lausanne, CH-1015 Switzerland

Abstract

Moissanite (natural SiC) has been recovered from podiform chromitites of several ophiolite complexes, including the Luobusa and Donqiao ophiolites in Tibet, the Semail ophiolite in Oman and the United Arab Emirates, and the Ray-Iz ophiolite of the Polar Urals, Russia. Taking these new occurrences with the numerous earlier reports of moissanite in diamondiferous kimberlites leads to the conclusion that natural SiC is a widespread mineral in the Earth's mantle, which implies at least locally extremely low redox conditions. The ophiolite moissanite grains are mostly fragments (20 to 150 μm) with one or more crystal faces, but some euhedral hexagonal grains have also been recovered. Twinned crystals are common in chromitites from the Luobusa ophiolite. The moissanite is rarely colorless, more commonly light bluish-gray to blue or green. Many grains contain inclusions of native Si and Fe-Si alloys ($FeSi_2$, Fe_3Si_7).

Secondary ion mass spectrometric (SIMS) analysis show that the ophiolite-hosted moissanite has a distinctive ^{13}C-depleted isotopic composition ($\delta^{13}C$ from -18 to -35 ‰, n= 36), much lighter than the main carbon reservoir in the upper mantle ($\delta^{13}C$ near -5‰). The compiled data from moissanite from

kimberlites and other mantle settings share the characteristic of strongly ^{13}C-depleted isotopic composition. This suggests that moissanite originates from a separate carbon reservoir in the mantle or that its formation involved strong isotopic fractionation. The degree of fractionation needed to produce the observed moissanite compositions from the main C-reservoir would be unrealistically large at the high temperatures required for moissanite formation. Subduction of biogenic carbonaceous material could potentially satisfy both the unusual isotopic and redox constraints on moissanite formation, but this material would need to stay chemically isolated from the upper mantle until it reached the high-T stability field of moissanite.. The origin of moissanite in the mantle is still unsolved, but all evidence from the upper mantle indicates that it cannot have formed there, barring special and local redox conditions. We suggest, alternatively, that moissanite may have formed in the lower mantle, where the existence of ^{13}C-depleted carbon is strongly supported by studies of extraterrestrial carbon (Mars, Moon, meteorites).

Keywords: moissanite, SIMS, C-isotopes, ophiolites, Ray-Iz, Luobusa, Dongqiao, Semail

1 Introduction

Moissanite, the natural form of silicon carbide, is named after Nobel Laureate Henri Moissan (chemistry, 1906), who reported SiC grains in the Canyon Diablo meteorite (Moissan, 1904). Although listed as "doubtful or incompletly described" in an overview of meteorite mineralogy by Mason (1967), moissanite has since been confirmed to exist in many meteorites, some extrasolar (e.g., Alexander, 1993 and references therein). Natural SiC has been reported as a rare accessory phase in a wide variety of terrestrial rocks since the 1960s (reviewed in Lyakhovich, 1980). The geologic community was at first slow to accept these findings because in most cases the moissanite was recovered from mineral separates and there was a possibility of contamination with synthetic SiC. Definitive proof of a natural origin came with the discovery of moissanite inclusions in diamond (Moore and Gurney, 1989; Otter and Gurney, 1989; Leung, 1990) from kimberlites, and such occurrences are now known from most cratons (South Africa, China, Siberia, North America, Brazil and Australia). In-situ occurrences of moissanite and/or intergrowths of moissanite with other natural minerals have also been documented in retrograde eclogites and serpentinites from the Dabie-Sulu belt in China (Qi et al., 2007; Xu et al., 2008) and in volcanic rocks (Bauer et al., 1963; Di Pierro et al., 2003; Zhang et al., 2006).

Probably the most frequently reported terrestrial host rock for moissanite is diamondiferous kimberlite, but is not clear if this has geological significance or if it simply reflects the fact that mineral concentrates from kimberlites are routinely scrutinized in detail. The compilation of moissanite occurrences by Lyakhovich (1980) shows an astonishing variety of host rocks including many of non-mantle origin like granites, salt deposits, limestones and bauxite. Accidental contamination by synthetic SiC may explain some of these occurrences, but it seems reckless to disclaim all of them, and in the case of moissanite from limestone (Gnoevaja and Grozdanov, 1965), a later study confirmed the occurrence using acid digestion where contamination can be ruled out (Shiryaev et al., 2008a). A surface origin of some moissanite is attested by its occurrence at meteorite impact craters (Ries: Hough et al., 1995; Berringer, Odessa: Miura et al., 1999) and in burn sites from forest fires (Sameshima and Rodgers (1990).

65 Here we report important new discoveries of moissanite from another geologic setting, namely,
66 magmatic chromitite bodies in the upper mantle section of ophiolites. The first report of moissanite and
67 diamond occurring in the ophiolite setting (Armenian Transcaucasus) is by Gevorkyan et al. (1976). Bai et
68 al. (2000) found moissanite and microdiamond in podiform chromitites from the Luobusa ophiolite, Tibet,
69 along with a number of other minerals which are interesting for their exotic stability conditions, requiring
70 ultrahigh pressure and/or very reducing environments (e.g., kyanite, coesite, metal alloys, native elements:
71 Bai et al., 2000; Robinson et al., 2004; Yang et al., 2007a). Motivated by the Luobusa finds, we have now
72 recovered moissanite from podiform chromitites and/or their peridotitic host, from the Dongqiao ophiolite
73 in Tibet, the Semail ophiolite in Oman and the Ray-Iz ophiolite in the Polar Urals of Russia (Fig. 1). In an
74 effort to understand the occurrence of SiC in ophiolites, and to compare these grains with those in
75 kimberlites, we determined C-isotope compositions of the ophiolite samples by in-situ secondary ion mass
76 spectrometry (SIMS). This investigation was motivated by the C-isotope studies of moissanite from
77 diamondiferous kimberlites by Leung et al. (1990) and Mathez et al. (1995), which found ^{13}C-depleted
78 compositions relative to the composition of most diamonds and other mantle-derived materials thought to
79 represent the dominant mantle carbon reservoir (δ^{13}C near -5‰; see Deines, 2002; Cartigny, 2005). It
80 turns out that the moissanite from all ophiolite localities sampled thus far have ^{13}C-depleted isotopic
81 compositions; and indeed, this appears to be a characteristic feature of all terrestrial moissanite that has
82 been studied to date (δ^{13}C from -18 to -35 ‰, n=72 from 12 occurrences).
83
84 **2 Geologic background**
85 The ***Luobusa ophiolite*** lies in the Yarlung-Zangbo suture in southern Tibet about 200 km ESE of
86 Lhasa (Fig. 1). It is a fault-bounded slab, 1-2 km thick, consisting largely of harzburgite that is believed to
87 have formed at a mid-ocean ridge at ~177 Ma and then been modified by boninitic melts above an
88 intraoceanic subduction zone at ~126 Ma (Zhou et al., 1996; 2005; Malpas et al., 2003; Yamamoto et al.,
89 2007). Luobusa hosts the largest active chromite mine in China. Numerous lenses and pods of chromitite

90 occur in the harzburgite where they are surrounded by envelopes of dunite formed by melt-rock reaction
91 in the upper mantle (Zhou et al., 1996; 2005). Our samples from orebodies 31 and 74 contain 80-90
92 volume % chromite with Cr# (100*Cr/Cr+Al) of 79-93 (Zhou et al., 1996). The Luobusa chromitites have
93 become well-known for the occurrence of ultra-high pressure minerals such as diamond and coesite
94 (IGCAGS, 1981; Robinson et al., 2004; Yang et al., 2007a).

95 The ***Dongqiao ophiolite*** is located in the Bangong Lake-Nujiang suture zone in central Tibet. It
96 consists of an 18-km-long block of harzburgite hosting lenses and pods of chromitite with compositions
97 similar to those of Luobusa (Cr# of 70-80: Shi et al., 2007). Amphibolites at the base of the ophiolite have
98 $^{40}Ar/^{39}Ar$ ages of 175-180 Ma (Zhou et al., 1997), suggesting formation in the Middle Jurassic. The bulk
99 sample from which SiC was separated originated from orebody Nr. 10.

100 The ***Semail ophiolite*** in Oman and the United Arab Emirates forms part of the Tethyan ophiolite belt
101 that extends from Europe through the Middle East to Tibet (e.g. Searle and Cox, 1999). Podiform
102 chromites occur in both the mantle transition zone and deeper in the mantle section (e.g., Ahmed and Arai,
103 2002; Rollinson, 2008), where they form small pods and lenses. We collected samples from two localities
104 in the Semail ophiolite. Sample OM-2 comes from the Shamis 2 orebody in Wadi Rajmi and consists of
105 massive chromite (Cr# = 64, (Rollinson, 2008) with interstitial olivine and orthopyroxene, minor
106 clinopyroxene and amphibole. Sample UAE-1 is massive chromite ore with minor olivine taken from a 1-
107 to 1.5-meter-thick chromitite lens in harzburgite from the defunct mine at Wadi Al-Hayl.

108 The **Ray-Iz ophiolite** occurs at the NE end of the Paleozoic Voikar-Syninsk ophiolite belt (Savel`ev
109 and Savel´yeva, 1977; Garuti et al., 1999; Yang et al., 2007b). A summary of age data in the ophiolite belt
110 (Savel´yeva et al., 2007) indicates early Ordovician to late Cambrian ages. The Ray-Iz ophiolite covers
111 over 400 km^2 and consists chiefly of tectonized harzburgite and dunite in the upper mantle section, with
112 minor amounts of gabbroic cumulates above the Moho. More than 200 podiform chromitite orebodies
113 occur, hosted chiefly in the harzburgite-dunite complex and consisting of high-Cr (Cr# = 0.74-0.86)
114 chromite (Pervozhikov et al., 1990).
115

2.1 Formation of podiform chromitites

Any attempt to explain the occurrence of moissanite in podiform chromitites must take into account the current models for the formation of these bodies. The mineralogical and geochemical-petrological features of podiform chromitites in the Luobusa, Dongqiao, Semail and Ray-Iz ophiolites are well established from previous work cited in the discriptions above. All are hosted by harzburgite in the upper mantle section and all are associated with dunite envelopes and veins. The favored model for massive chromite formation in this setting is a sudden chromite precipitation from basaltic (or boninitic) melts triggered by melt-rock interaction that produced the dunite veins and envelopes (Zhou et al., 1996). Many of the chromitites and associated dunites show evidence of brittle fracture, supporting the litho-stratigraphic evidence for formation at shallow depths (Zhou et al., 1996; Robinson et al., 2004). There is no doubt that in these ophiolites, the chromitite bodies accumulated at shallow mantle depths, but the occurence of high-pressure minerals within them is highly enigmatic. The high-pressure phases like diamond or coesite (Yang et al., 2007a) presumably occur as inclusions in the chromite, and it is impossible to conceive that they could survive in a low-pressure basaltic melt crystallizing chromite, without some kind of armoring. One possibility is that the chromite grains hosting such high-pressure minerals are xenocrysts themselves and were transported by upwelling mantle and/or partial melts from much greater depths. Evidence for xenocrystic chromites was suggested based on observed Re-Os ages of chromitites that predate the host ophiolite at Dongqiao (Shi et al., 2007), and by the finding of coesite and clinopyroxene lamellae in chromite grains from Luobusa (Yamamoto et al., 2008), which requires crystallization of the host at high pressure. Clearly, this new evidence makes it easier to understand the finding of diamond and other high-pressure or chemically incompatible phases in mineral separates from these chromitites, and there may be implications for the formation of chromite ores more generally, but these are still isolated observations and there is no information yet available on how widespread xenocrystic chromite in ophiolites may be.

3 Sample descriptions

Moissanite is a rare mineral and our procedures for sampling and sample treatment were designed accordingly. Very large samples of chromite ore, 100 to 500 kg each, were collected from outcrops at mine sites. In the processing facility the samples were first cleaned, then ground to pass a 1 mm mesh sieve using machinery free of SiC components (steel jaw-crushers, steel ball or roller mills). Heavy minerals were separated using gravimetric and magnetic techniques, and moissanite was hand-picked from these separates under a binocular microscope. Mineral identification was based on optical properties and confirmed by Raman spectroscopy, SEM-EDS or X-ray diffraction. Although the studied grains were recovered from mineral separates, we are confident that the material reported is natural moissanite for the following reasons: (1) samples were collected directly from outcrop; (2) sample preparation (crushing and mineral separation) was done at different occasions in different laboratories: Freiberg, Saxony, the GFZ Potsdam and St. Petersburg for the Oman samples, and Zhengzhou, China, for Luobusa and Donqiao. Care was taken to avoid contamination during all stages of sampling and processing. The machinery was disassembled and carefully cleaned before use and none of the components used in processing contained SiC. In the case of Luobusa chromitite, a 100 kg sample of granite was processed before the chromitite in exactly the same way and went through the same mineral separation procedure but not one grain of SiC was found; (3) moissanite from Luobusa is intergrown with and/or contains inclusions of the Ca-Al phase gehlenite (Hu, 1999), which was also found along with anorthite, in moissanite from Turkey by Di Pierro et al., (2003). To the authors' best knowledge, Ca-Al silicates have never been reported from synthetic SiC.

The moissanite grains recovered in this study are mostly conchoidal fragments (20 to 150 μm), probably produced during sample preparation. Some euhedral hexagonal grains were also recovered and many of the broken grains show one or more well-developed crystal faces. Some moissanite from the Luobusa ophiolite forms twinned crystals (Fig. 2). The moissanites are rarely colorless, more commonly light blue-gray to blue or green. Electron microprobe analyses for Al, Fe, Sc, Cr using enhanced counting times to improve sensitivity failed to find significant concentrations in most grains but in other cases, Al and Fe contents of up to 300 ppm have been reported (cf. Bauer et al., 1963; Marshintsev, 1990; Mathez et al., 1995; Shiryaev et al., 2008a). Some of the moissanite grains from the Semail, Luobusa and Ray-Iz

ophiolites contain rounded inclusions of native Si and, more rarely of Fe-Si alloys (Fig. 3b,c). In our example and in other published reports, the Fe-Si phase occurs at the boundary of native Si and the SiC host (Mathez et al., 1995; Di Pierro et al., 2003; Shiryaev et al., 2008a). The Fe silicides in our example are too small for electron microprobe analysis because of beam overlap with the SiC host, but analyses of individual Fe-Si grains from Luobusa revealed Fe_3Si_7 and $FeSi_2$ (Bai et al. (2000).

The association of moissanite and native Si, with or without Fe-silicides, appears to be characteristic since it has been found in most studied moissanite localities (Marshintsev, 1990; Leung et al., 1990; Mathez et al., 1995; di Pierrro et al., 2003; Shiryaev et al., 2008; Xu et al., 2008). The Si inclusions are typically round (Fig. 2), which suggest a trapped melt. If so, this places limits on the trapping conditions. The melting point of Si (1410°C at surface) decreases with pressure by about -33°/GPa (Soma and Matsuo, 1982), so Si metal should be liquid at mantle depths below about 200 km (for the continental mantle geotherm).

4. Carbon isotope compositions

4.1 Methods

Carbon isotope analyses were performed on polished, gold-coated grain mounts of moissanite using a Cameca ims6f secondary ion mass spectrometer (SIMS). The analyses employed a $^{133}Cs^+$ primary beam operated at 400 pA and 10 kV, and a secondary extraction voltage of -7.5 kV with an energy window of 50 eV and no energy offset. A 20 μm contrast aperture was used in conjunction with a 750 μm field aperture (60 μm field of view). The mass resolving power of $M/\Delta M \approx 3700$ was adequate to resolve ^{13}C from the isobaric interference by $^{1}H^{12}C$. The conductivity of SiC made electron flooding unnecessary. The beam diameter at the sample surface was ~5 μm. Each analysis consisted of a 10 minute preburn followed by 80 cycles of the peak stepping sequence - mass 11.9 (background, 0.1 s per cycle), ^{12}C (2 s) and ^{13}C (5 s). A deadtime correction of 16 ns was applied to all data. SIMS analyses were performed on 2-5 grains from each of the localities, giving a total of 36 analyses (Table 2). Carbon isotope compositions are reported as $\delta^{13}C = \{^{13}C/^{12}C_{sample} / {}^{13}C/^{12}C_{RM} - 1\} \times 1000$) relative to the PDB reference ($^{13}C/^{12}C =$

193 0.0112372). Instrumental mass fractionation and analytical uncertainties were monitored using two
194 synthetic SiC reference materials: ANMH 100578 (Mathez et al., 1995), and an in-house reference
195 prepared from 80-mesh SiC abrasive (GFZ-S113). The C-isotope composition of ANMH 100578 is
196 slightly uncertain because the procedure used in combusting the SiC resulted in yields of less than 50%
197 (Mathez et al., 1995). The C-isotope composition of our in-house reference material GFZ-S113 was
198 determined at the University of Lausanne using procedures described in detail in the appendix. Yields
199 were between 90 and 100% for each of two duplicate analyses of the GFZ-S113 material, and the resulting
200 $\delta^{13}C$ values are –28.71 and –28.79‰. Mathez et al. (1995) noted that their C-isotope determination for
201 ANMH 100578 could be affected by the incomplete yield of sample combustion, but the agreement of
202 both reference materials in our study show that this is not the case (Table 1). Based on repeated analyses
203 of the reference materials (Table 1) the internal precision of our SIMS measurements is about 1 per mil
204 and the repeatability is about 2 per mil (1 σ values).
205 We also conducted SIMS analyses on moissanite grains separated from the Turkish volcanic pebble
206 previously studied by Di Pierro et al. (2003). The average of 9 analyses performed on the Turkish
207 moissanite is -26.7 ‰, which agrees very well with the value of -28 ‰ reported in the earlier study.
208 However, the range of $\delta^{13}C$ values in the SiC grains is from -21 to -31 ‰ (Table 2), and even the within-
209 grain variations are up to 9 ‰. This heterogeneity went unnoticed in the earlier study because C analysis
210 was done on an aggregate sample by conventional mass spectrometry.
211
212
213
214 **4.2 Results**
215 The total range of $\delta^{13}C$ values from ophiolite-hosted moissanite is -18 ‰ to -35 ‰ (Table 2, Fig. 3).
216 The mean value and standard deviation of 27 analyses comprising four localities are -28.2 ± 3.9 ‰. A
217 comparison of results for the four ophiolite localities Ray-Iz (-32.7 ± 2.1 ‰), Luobusa (-28.4 ± 3.3 ‰),

218 Dongqiao (-23.5 ± 3.4 ‰) and Semail (-28.1 ± 2.6 ‰) shows considerable overlap, with only two
219 localities: Ray-Iz and Dongqiao being statistically distinguishable. The range of C-isotope compositions
220 within each locality varies from 5 to 9 ‰, which is larger than analytical uncertainty even at the 2-sigma
221 level (4 ‰). Typically, only a single spot on each moissanite grain was analysed in order to maximize the
222 sample coverage and thus we have no information on within-grain variations for most samples.
223 Exceptions are one grain from the Semail ophiolite (UAE1-2) and one from Luobusa, which were
224 analyzed twice and showed less than 3 ‰ variation (Table 2). In their SIMS study of mosssanite from two
225 kimberlites in Yakutia, Mathez et al. (1995) found a range of $\delta^{13}C$ values of about 4 ‰ for the individual
226 localities Aihkal and Mir. Those authors mentioned a weak correlation of the C-isotope composition with
227 color of moissanite grains, but no such correlation was observed for the ophiolite moissanite in our study
228 (Table 2). Shiryaev et al. (2008b) determined a range of about 3.5 ‰ among different moissanite grains
229 from Yakutia kimberlites and inferred possible growth zoning but this is not demonstrable from their data
230 coverage. Lacking more within-grain analyses and petrographic association we can offer no comment on
231 the significance of C-isotope variations observed our study.
232 The most important result in our C-isotope study is that all moissanites from the studied ophiolites are
233 strongly depleted in ^{13}C relative to the mantle carbon reservoir represented by diamonds, carbonatites,
234 mantle xenoliths and CO_2 emissions from basaltic volcanoes with $\delta^{13}C$ value around -5 ‰, as reviewed by
235 Deines (2002). Furthermore, a data compilation of published C-isotope analyses of natural moissanite
236 from the other settings (Fig. 3) shows that all terrestrial occurrences of moissanite yet described contain
237 carbon that is strongly depleted in ^{13}C. As pointed out earlier (Mathez et al., 1995; Di Pierro et al., 2003),
238 and confirmed by our study (Table 1), synthetic SiC has low $\delta^{13}C$ values in the same range as the natural
239 mineral. Therefore, one cannot use carbon isotope compositions alone to distinguish natural from
240 synthetic SiC. This does not refute our claim of a natural origin for the moissanites studied, for which
241 other evidence was described above. Note also that Leung et al. (1990) found ^{13}C-depleted carbon ($\delta^{13}C$-
242 24 ‰) in moissanite inclusions in diamond from the Fuxian kimberlites, which are undeniably natural.

243 The host diamonds in that example yielded $\delta^{13}C$ values of -2.9 to -4.5‰, within the "normal" mantle
244 range.
245
246 **5 Discussion**
247 With the new occurrences reported here, moissanite is now well documented from mantle-derived
248 rocks of both the kimberlite-lamproite association (sub-cratonic lithosphere) and the ophiolite association
249 (shallow upper mantle). In both cases, its occurrence is enigmatic because the low redox conditions
250 required for SiC formation seem highly incompatible with the geologic settings in which it is found. The
251 extremely reducing environment of formation is underscored by the common presence of native Si
252 inclusions within moissanite grains. A second enigmatic feature of moissanite from the earth's mantle is
253 the rather narrow range of C-isotopic composition from all occurrences yet studied, and the fact that these
254 compositions are strongly ^{13}C-depleted compared with most diamonds and other carbon-bearing phases
255 known from the mantle. It may be that the unusual redox conditions and isotopic composition of
256 moissanite are both related to how the mineral forms in Earth, but we first consider the two characteristics
257 separately.
258
259 **5.1 Redox conditions and moissanite formation**
260 The redox conditions in the upper mantle are well established by many lines of evidence, and lie
261 within one or two log units of the forsterite-magnetite-quartz (FMQ) buffer (see review by Frost and
262 McCammon, 2008). Certainly in the shallow upper mantle where ophiolites are formed, particularly in
263 suprasubduction zone settings, one can expect conditions near the FMQ buffer. Studies of mineral
264 inclusions in kimberlitic diamonds indicate that the great majority grew at the base of thick mantle
265 lithosphere between about 140 and 200 km depth with exceptional cases suggesting formation in the
266 mantle transition zone (410 to 660 km) or the shallow part of the lower mantle (Stachel et al., 2005).
267 Oxygen fugacity estimates vary but many diamonds appear to have formed at fO_2 conditions around the
268 iron-wüstite (IW) buffer (Jacob et al., 2004).

269 The redox stability of moissanite was estimated from thermodynamic analysis by Essene and Fisher
270 (1986) and by Mathez et al. (1995), and was studied experimentally by Ulmer et al. (1998). All of these
271 studies conclude that moissanite formation requires oxygen fugacities several orders of magnitude lower
272 than that of the iron-wüstite buffer. Ulmer et al. (1998) found no important change in the relative positions
273 of metal-oxide buffers and moissanite-forming reactions to pressures as high as 9 GPa. Dobrzhinetskaya
274 and Green (2007) produced moissanite during diamond synthesis experiments in a graphite-silicate system
275 with fO_2 conditions nominally at the iron-wüstite buffer (1450-1500°C, 8.5 GPa). The authors took the
276 formation of moissanite to mean that their oxygen fugacity was much lower than intended, but it is also
277 possible that moissanite stability at high pressure needs further scrutiny. However, the common
278 occurrence of native Si inclusions in natural moissanite supports the inference of redox conditions far
279 below the iron-wüstite buffer. Experiments and calculations of Fe and Si metal-oxide equilibria by
280 Malavergne et al. (2004) place the Si-SiO_2 buffer about 8 log units below the iron-wüstite buffer at 20
281 GPa and 2000°C, and the difference between the two buffers increases at lower temperature.
282 Stable growth of moissanite in the upper mantle can therefore be ruled out unless there are special
283 redox conditions (see below). The bulk chemical composition and redox conditions of the lower mantle
284 are not known from direct observation on xenoliths or igneous rocks, and it is not clear whether SiC and
285 other reduced phases like metallic Si would be stable under "normal" lower mantle conditions, but
286 prevailing thermodynamic and mineralogic models would suggest not. Frost and McCammon (2008)
287 calculated the depth variations in oxygen fugacity for a 4-phase garnet peridotite along the cratonic
288 geotherm. According to this model, there is a steady decrease of fO_2 with depth until the IW buffer is
289 intersected at about 8 GPa, but once Fe-Ni alloy forms, further decrease in fO_2 with depth is small and
290 conditions of 5 or more log units below IW are not achieved anyhere in the lower mantle. The metastable
291 extension of Frost and McCammon´s P-fO_2 relation without Fe-saturation reaches fO_2 values 5 log units
292 below IW at around 25 GPa. However, this seems an unrealistic proposition based on work by Rohrbach
293 et al. (2007) and given that Fe-Ni alloys are relatively common in mineral separates from the ophiolite
294 chromitites we have studied (e.g., Bai et al., 2000; Robinson et al., 2004; Shi et al., 2007).

295 In summary, the available evidence suggests that conditions are too oxidizing for moissanite (and
296 native Si) formation in the upper mantle. Conditions in the lower mantle also seem hostile to moissanite
297 stability from current understanding, but this is much less certain. The alternative is to propose local,
298 highly reducing microenvironments in the mantle. One well-known example of this kind in the upper
299 mantle is the local reduction of Fe-silicates to form Fe-Ni metal (awaruite) due to release of H_2 during
300 serpentinization (e.g., Dick, 1974; Sleep et al., 2004). The high temperatures required for moissanite to
301 form rule out this specific explanation for SiC, but there can be analogous hydration reactions at higher P
302 and T involving DHMS phases (dense hydrous magnesian silicates), which are known to be stable above
303 22 GPa and 1200°C (Ohtani et al., 2001). Another example of a reducing microenvironment was proposed
304 by Jacob et al. (2004) to explain their finding of FeC and native Fe inclusions in diamonds. They
305 suggested that local and transient reducing conditions result from production of hydrogen when diamond
306 grows from a methane-dominated fluid (see also Thomassot et al., 2007). This explanation encounters
307 problems when considering the distinctly different C-isotope compositions of moissanite and diamonds as
308 described in the following section. A possibility suggested by Mathez et al. (1995) is that subducted
309 carbonaceous sediment from the surface could create a reducing microenvironment in the mantle if it
310 could remain intact. This may be unlikely, but it has the attraction of also explaining the distinctive C-
311 isotope composition of moissanite (see below).
312
313
314 **5.2 The carbon isotope perspective**
315 Reviews of the isotopic composition of carbon in mantle xenoliths, magmatic rocks and related fluids
316 by Deines (2002), and of diamonds by Cartigny (2005) establish that the dominant mantle carbon
317 reservoir sampled by these materials has a $\delta^{13}C$ value near -5 ‰. Our new SIMS results from moissanite
318 in ophiolites, and the compilation of published C-isotope compositions of moissanite from other settings
319 (Fig. 3) show that all terrestrial moissanites analyzed thus far are strongly ^{13}C-depleted relative to this
320 value. Mathez et al. (1995) pointed out this isotopic feature of moissanite based on the then-available 30

analyses, and it remains valid now with more than twice as much data. Considerably more data on the stable isotope composition of diamonds are also now available and we briefly summarize what is known about ^{13}C-depleted carbon in the mantle from the diamond perspective. Of the more than 4400 C-isotope analyses compiled in the review by Cartigny (2005), 72% have a narrow range of δ^{13}C values from -8 and -2 ‰, and these are attributed to the main C reservoir in the mantle. From the remainder, a few analyses are enriched in ^{13}C (to a maximum of +5 ‰), but the great majority are ^{13}C-depleted, with a minimum value of -38.5 ‰. Several features of these ^{13}C-depleted diamonds (based on Galimov, 1991; Kirkley et al., 1991; Deines, 2002, Cartigny, 2005 and Heaney et al., 2005) are worth emphasizing:

1. Most crustal-derived microdiamonds from deeply-subducted ultra-high pressure (UHP) metamorphic terranes have ^{13}C-depleted compositions. A compilation of 120 δ^{13}C values from UHP metamorphic diamonds by Cartigny (2005), shows a range from -4 to -30 ‰ with a broad peak around -10 ‰. Microdiamonds from the Erzgebirge UHP terrane in Germany have more restricted δ^{13}C range of -17 to -29 ‰ (Dobrzhinestskaya et al., 2007). The ^{13}C-depleted composition of these diamonds is logically attributed to biogenic carbon in the protoliths, although as Horita (2005) discuss, abiogenic processes can produce the same degree of isotopic fractionation as biogenic ones (see also discussion of ^{13}C-depleted Hadean microdiamond and graphite from Jack Hills, Australia, by Nemchin et al., 2008).
2. All grains of the enigmatic, polycrystalline variety of diamond called carbonado have ^{13}C-depleted compositions in the δ^{13}C range of -23 to -30 ‰. The origin of carbonado diamonds is a major puzzle but several features suggest a crustal setting (Heaney et al., 2005). Interestingly, moissanite is among the inclusion phases reported from carbonados (Heaney et al., 2005).
3. Among kimberlitic diamonds, ^{13}C-depleted compositions (δ^{13}C < -10 ‰) are proportionally much more common in eclogite-types (34%) than in peridotite-type diamonds (2%)
4. Kimberlitic diamonds with ^{13}C-depleted compositions (δ^{13}C < -10 ‰) have a wide range of δ^{13}C values, and compositions from individual localities can be distinctly different (Galimov, 1991).

346

347 The reason(s) forC-isotope heteogeneity and ^{13}C-depleted composition of diamonds is the subject of
348 lengthy discussion (see Galimov, 1991: Kirkley et al., 1991; Deines, 2002; Cartigny, 2005), which centers
349 around three options: i) introduction of surface-modified, biogenic carbon into the mantle by subduction,
350 ii) intrinsic heterogeneity of mantle carbon, and iii) isotopic fractionation of C from a once-homogeneous
351 reservoir. Different authors have favored one scenario over another but most conclude that multiple
352 carbon sources are required to explain the compositional range of all ^{13}C-depleted diamonds.

353 The above scenarios for explaining ^{13}C-depleted diamonds are also relevant for the interpretation of
354 moissanite compositions, but the moissanite situation is special in several ways. One distinction is the
355 extremely low oxygen fugacity required for moissanite stability and for its inclusions of Si and Fe-Si
356 alloy. Another important distinction is the relatively narrow range and low values of $\delta^{13}C$ from
357 moissanites (-18 to -35 ‰) compared with those of ^{13}C-depleted diamonds (Fig. 3), excepting carbonado
358 (-23 to -30 ‰; Heaney et al., 2005). One possible explanation for the distinctive and rather homogeneous
359 ^{13}C-depleted composition of natural moissanite is a systematic isotopic fractionation from an equally
360 homogeneous carbon source, i.e., the mantle reservoir at -5 ‰. The fractionation hypothesis has been
361 widely discussed with respect to ^{13}C-depleted diamonds and found to be lacking (Cartigny, 2005), and the
362 same problems apply for SiC. Equilibrium C-isotope fractionation between diamond and CO_2 or CH_4 at
363 high temperatures are about 4 ‰ and 1 ‰, much too small to explain the $\delta^{13}C$ variations from a single
364 starting composition of -5 ‰. A greater shift in isotopic composition could be achieved by open-system
365 fractionation where one C component is continuously removed. However, modeling of this process
366 (Deines, 1980) shows that it would result in a skewed distribution of $\delta^{13}C$ values quite unlike the narrow
367 range in moissanite, and nowhere near the observed low values of around -30 ‰. Experimental
368 fractionation studies involving SiC are lacking, but we can still expect low fractionation factors at high
369 temperature and a continuous distribution of $\delta^{13}C$ values resulting from open-system processes.

370 If the ^{13}C-depleted composition of moissanite cannot be produced by fractionation from the carbon
371 reservoir in the mantle with -5 ‰, then there must be at least one other, isotopically distinct source of
372 carbon, which is either introduced from the crust via subduction or is inherent to the mantle. The C-
373 isotopic composition of moissanite overlaps closely with the range of biogenic carbon and as noted above,
374 the subduction of carbonaceous material could satisfy both the isotopic and the redox constraints for
375 moissanite formation. As Mathez et al. (1995) pointed out, it would be difficult to avoid dilution and
376 oxidation of the carbonaceous component during subduction-zone metamorphism and deformation before
377 reaching the high-temperature conditions (>1000° C) needed for moissanite formation. Subduction of
378 biogenic carbon cannot be completely ruled out, but it is not an easy explanation because of the need to
379 chemically isolate the special microenvironment through the subduction process.
380 The alternative hypothesis to subduction of an appropriately light carbon source is that the mantle
381 inherently contains more than one isotopically distinct carbon reservoir. This is a view widely held among
382 diamond researchers (e.g., Deines, 2002; Cartigny, 2005), and the best evidence for indigenous ^{13}C
383 depleted carbon comes from studies of extraterrestrial carbon. The C-isotope variability in meteorites is
384 often cited as evidence that the accreted earth did not have a homogeneous bulk composition of -5 ‰
385 (e.g., Kirkley et al., 1991; Deines, 2002; Rollinson, 2007). An important piece of evidence in this regard
386 comes from a study of carbon in Mars meteorites by Grady et al. (2004). They reported $\delta^{13}C$ values of -20
387 ±4 ‰ for 12 Mars meteorites, suggesting the Martian mantle may have been uniformly ^{13}C-depleted.
388 Furthermore, Kashizume et al. (2004) suggested that solar carbon must be isotopically light ($\delta^{13}C < 100 \pm$
389 20‰) based on SIMS analysis of solar wind-implanted C in the lunar regolith.
390 There is abundant, good evidence for a major carbon reservoir in the Earth's mantle with $\delta^{13}C = -5$ as
391 mentioned above, but that is based on materials from intermediate (rarely) to upper mantle (mostly)
392 depths. If we accept the extraterrestrial evidence that the bulk Earth, like Mars, had a more ^{13}C-depleted
393 composition, then the prevelance of C-isotope values around -5 ‰ in the upper mantle implies a deeper
394 reservoir of lighter carbon. It is speculative but certainly possible, that the moissanite C-isotope

composition reflects a deep-mantle origin. The source region for moissanite has the additional constraint of very low oxygen fugacity (although the two conditions need not be directly related). As discussed in the previous section, robust estimates of oxygen fugacity in the mantle are limited to the relatively shallow depths from which there is observational evidence, and it is certain that moissanite cannot stably form there. The lower mantle redox conditions are not known to be appropriate for moissanite formation but they are model-dependent and much less certain.

The ultimate origin of moissanite found in our ophiolite samples and in kimberlites remains unanswered, however we argue that there is a good possibility that moissanite in mantle-derived rocks originates in the lower mantle. For this reason alone, natural miossanites are worth further critical study. More insights may from application of other isotopic systems (N, Si) to moissanite collections already available. For example, Mathez et al. (1995) reported two N-isotope determinations from kimberlite-hosted moissanite ($\delta^{15}N$ = 9.7 ‰ and 5.6 ‰). These values are at the heavy end of the upper mantle range (-25 to +15 ‰) and overlap with metamorphic diamonds and N from metasediments (Cartigny, 2005). More studies of this kind would be helpful but it is also important that further occurrences of moissanite be actively explored and investigated.

6 Conclusions

We have shown that moissanite is a relatively common mineral in podiform chromitites and/or host peridotite from four ophiolites of different age and geographic location (Luobusa and Dongqiao in Tibet, Ray-Iz in the Polar Urals and Semail in the Arabian peninsula). Our results, combined with previously published data firmly demonstrate the existence of natural SiC as a rare but rather widespread mineral in Earth's mantle. In the chromitites, moissanite is associated with a wide variety of unusual minerals including diamonds, coesite, kyanite, Fe-Si alloys and native elements. Many moissanite grains from both ophiolites and kimberlites contain inclusions of native Si and Fe-silicides. The rounded form of these inclusions suggests formation as trapped liquids. The redox and temperature conditions implied by these inclusions are compatible with the stability conditions for moissanite, but are not compatible with the

421 conditions expected either in the ophiolite or in the kimberlite source regions of the upper mantle. We
422 conclude that the ophiolitic moissanite grains are xenocrysts that have been incorporated into the
423 chromitites, though the possibility of deep origin for some of the chromitite is indicated by a recent
424 finding of coesite lamellae in chromite grains from the Luobusa ophiolite (Yamamoto, et al., 2009).
425 All of the ophiolite-hosted moissanite grains have a distinctive and narrow range of ^{13}C-depleted
426 isotopic compositions (-18 to -35 ‰), and this same range applies to all natural moissanite studied thus
427 far. The C-isotope composition of moissanite is thereby distinct from that of kimberlitic diamonds, even
428 those of the ecologite-type. It is not possible to explain the ^{13}C-depleted range of moissanite by isotopic
429 fractionation from the mantle carbon reservoir with a δ^{13}C value of -5 ‰, with or without Rayleigh
430 distillation. Moissanite, like some ^{13}C-depleted diamonds, must tap a separate carbon reservoir in the
431 mantle. There is good evidence from studies of extraterrestrial materials that ^{13}C-depleted carbon was
432 incorporated in the early Earth, so the observed prevalence of upper mantle δ^{13}C values near -5 ‰, implies
433 the existence of isotopically lighter carbon in a deeper reservoir. The ultimate source of moissanite from
434 the ophiolite and kimberlite associations is still unknown but a lower mantle origin is one of the better
435 possibilities and it should be futher explored.
436 .
437
438 **Acknowledgements**
439 We thank E. Mathez, AMNH for providing a sample of ANMH 100578 reference SiC. D. Rhede, R.
440 Wirth and M. Gottschalk, GFZ, are gratefully acknowledged for their assistance with electron microprobe,
441 TEM and XRD analyses, respectively. Thanks also go to A. Shiryaev, I. Veksler and R. Wirth for their
442 very helpful discussions. Journal reviews by L. Dobrzhinetskaya and H. Rollinson were most helpful.
443 Hugh Rollinson pointed out the possible significance of C-isotopes in the Mars meteorites.
444
445

446 **References**

447 Alexander, C. M. O., 1993. Presolar SiC in chondrites: how variable and how many sources? Geochimica
448 et Cosmochimica Acta 57, 2869-2888

449 Ahmed, A. H., Arai, S., 2002. Unexpectedly high-PGE chromitite from the deeper mantle section of the
450 northern Oman ophiolite and its tectonic implications. Contributions to Mineralogy and Petrology
451 143, 263-278.

452 Bai, W.-J., Robinson, P. T., Fang, Q.-S., Yang, J.-S., Yan, B.-G., Zhang, Z.-M., 2000. The PGE and base-
453 metal alloys in the podiform chromitites of the Luobusa ophiolite, southern Tibet. Canadian
454 Mineralogist 38, 585-598.

455 Bauer, J., Fiala, J., Hrichová, R., 1965. Natural α-silicon carbide. American Mineralogist 48, 620-634.

456 Cartigny, P., 2005. Stable isotopes and the origin of diamond. Elements 1, 79-84.

457 Deines, P., 1980. The carbon isotopic compositions of diamonds: relationship to diamond shape, color,
458 occurrence and vapor composition. Geochimica et Cosmochimica Acta 44, 943-961.

459 Deines, P., 2002. The carbon isotope geochemistry of mantle xenoliths. Earth Science Reviews 58, 247-
460 278.

461 Dick, H. J. B., 1974. Terrestrial nickel iron from the Josephine Peridotite, its geologic occurrence,
462 associations, and origin. Earth and Planetary Science Letters 24, 291-298.

463 Di Pierro, S., Gnos, E., Grobéty, B. H., Armbruster, T., Bernasconi, S. M., Ulmer, P., 2003. Rock-forming
464 moissanite (natural α-silicon carbide). American Mineralogist 88, 1817-1821.

465 Dobrzhinetskaya, L. A., Green, H. W., II, 2007. Diamond synthesis from graphite in the presence of
466 water and SiO2: Implications for diamond formation in quartzites from Kazakhstan. International
467 Geology Review 49, 389-400.

468 Dobrzhinetskaya, L. A., Wirth, R., Green, H. W., II, 2007. A look inside of diamond-forming media in
469 deep subduction zones. Proceedings of National Academy of Sciences of the United States of America
470 104, 9128-9132.

Essene, E. J., Fisher, D. C., 1986. Lightning strike fusion: extreme reduction and metal-silicate liquid immiscibility. Science 234, 189-193

Fang, Q.-S., Bai, W.-J., 1981. The discovery of Alpine-type diamond-bearing ultrabasic intrusions in Tibet. Geological Review 22, 455-457.

Frost, D. F., McCammon, C. A., 2008. The redox state of Earth's mantle. Annual Review of Earth and Planetary Sciences 36, 389-420.

Galimov, E. M., 1991. Isotope fractionation related to kimberlite magmatism and diamond formation. Geochimica et Cosmochimica Acta 55, 1697-1708.

Garuti, G., Zaccarini, F., Moloshag, v., Alimov, V., 1999. Platinum-group minerals as indicator of sulfur fugacity in ophiolitic upper mantle: an example from chromitites of the Ray–Iz ultramafic complex (Polar Urals, Russia). Canadian Mineralogist 37, 1099-1115

Gevorkyan, R. G., Kaminsky, F. V., Lunev, V. C., Osovetsky, V. M., Nachatryan, N. D., 1976. A new occurrence of diamonds in ultramafic rocks in Armenia, Doklady AN Armenian SSR 63, 176–181.

Gnoevaja, N., Grozdanov, L., 1965. Moissanite from Triassic rocks, NW Bulgaria. Proceedings of the Bulgarian Geological Society 26, 89-95.

Gorshkov, A. I., Bao, Y. N., Bershov, L. V., Ryabchikov, I. D., Sivtsov, A. V., Lapina, M. I., 1997. Inclusions of native metals and other minerals in diamond from Kimberlite Pipe 50, Liaoning, China. International Geology Review 8, 794-804.

Grady, M M., Verchovsky, A. B., Wright, I. P., 2004. Magmatic carbon in Martian meteorites: attempts to constrain the carbon cycle on Mars. International Journal of Astrobiology 3, 117-124.

Heaney, P. J., Vicenzi, E. P., De, S., 2005. Strange diamonds: the mysterious origins of carbonado and framesite. Elements 1, 85-89.

Horita, J., 2005. Some perspectives on isotope biosignatures for early life. Chemical Geology 218, 171-186.

496 Hough, R. M., Gilmour, I., Pillinger, C. T., Arden, J. W., Gilkes, K. W. R., Juan, J., Milledge, H. J., 1995.
497 Diamond and silicon carbide in impact melt rock from the Ries impact crater. Nature, 387, 41-44.
498 Hu, X.-F., 1999. Origin of diamonds in chromitites of the Luobusa Ophiolite, southern Tibet, China. MSc
499 Thesis, Dalhousie University, Halifax, Nova Scotia, Canada, 151 pp.
500 Institute of Geology, Chinese Academy of Geological Sciences (IGCAGS), 1981. The discovery of
501 Alpine-type diamond-bearing ultrabasic intrusions in Xizang: Geological Review, 22, 455-457.
502 Jacob, D. E., Kronz, A., Viljoen, K. S., 2004. Cohenite, native iron and troilite inclusions in garnets from
503 polycrystalline diamond aggregates. Contributions to Mineralogy and Petrology 146, 566-576.
504 Kashizume, K., Chaussidon, M., Marty, B., Terada, K., 2004. Protosolar carbon isotope composition:
505 implications for the origin of meteoritic organics. The Astrophysical Journal 600, 480-484.
506 Kirkley, M. B., Gurney, J. J., Otter, M. L., Hill, S. J., Daniels, L. R., 1991. The application of carbon
507 isotope measurements to the identification of the sources of C in diamonds: a review. Applied
508 Geochemistry 6, 477-494.
509 Leung, I., 1990. Silicon carbide cluster entrapped in a diamond from Fuxian, China. American
510 Mineralogist 75, 1110-1119.
511 Leung, I., Guo, W., Friedman, I., Gleason, J., 1990. Natural occurrence of silicon carbide in a
512 diamondiferous kimberlite from Fuxian. Nature 346, 352-354.
513 Lyakhovich, V. V., 1980. Origin of accessory moissanite. International Geology Review 22, 961-970.
514 Malavergne, V., Siebert, J., Guyot, F., Gautron, L., Combes, R., Hammouda, T., Borensziajn, S., Frost, D.,
515 Martinez, I., 2004. Si in the core? New high-pressure and high-temperature experimental data.
516 Geochimica et Cosmochimica Acta 68, 4201-4211.
517 Malpas, J, Zhou, M.-F., Robinson, P. T., Reynolds, P. H., 2003. Geochemical and geochronological
518 constraints on the origin and emplacement of the Yarlung-Zangbo ophiolites, southern Tibet.
519 Geological Society London, Special Publication 218, 191-206.
520 Mason, B., 1967. Extraterrestrial mineralogy. American Mineralogist, 52, 307-325.

521 Marshintsev, V. K., 1990. Natural silicon carbide in Yakutian kimberlites. Mineralogicheskii Zhurnal 12,
522 17-26 (in Russian).
523 Mathez, E. A., Fogel, R. A., Hutcheon, I. D., Marshintsev, V. K., 1995. Carbon isotope composition and
524 origin of SiC from kimberlites of Yakutia, Russia. Geochimica et Cosmochimica Acta 59, 781-791.
525 Miura, Y., Kobyashi, H., Kedves, M., Gucsik, A., 1999. Carbon source from limestone targets by impact
526 reaction at the K/T boundary. 30th Lunar and Planetary Science Conference Proceedings, Houston,
527 1522.
528 Moissan, H., 1904. Nouvelles recherches sur la météorité de Cañon Diablo. Comptes Rendus 139, 773–
529 786 (in French).
530 Moore, R. O., Gurney, J. J., 1989. Mineral inclusions in diamond from the Monastery kimberlite, South
531 Africa. Geological Society of Australia Special Publication 14, 1029-1041.
532 Nemchin, A .A., Whitehouse, M. J., Menneken, M., Geisler, T., Pidgeon, R. T., Wilde, S. A., 2008. A
533 light carbon reservoir recorded in zircon-hosted diamond from the Jack Hills. Nature 454, 92-95.
534 Ohtani, E., Toma, M., Litasov, K., Kubo, T., Suzuki, A., 2001. Stability of dense hydrous magnesium
535 silicate phases and water storage capacity in the transition zone and lower mantle. Physics of the Earth
536 and Planetary Interiors 124, 105-117.
537 Otter, M. L., Gurney, J. J., 1989. Mineral inclusions in diamonds from the Sloan diatreme, Colorado-
538 Wyoming state line kimberlite district, North America. Geological Society of Australia Special
539 Publication 14, 1042-1053.
540 Qi, X. X., Yang, J. S. Xu. Z. Q., Bai, W. J., Zhang, Z. M., Fang, Q. S., 2007. Discovery of moissanite in
541 retrogressive eclogite from the Pre-pilot hole of the Chinese Continental Scientific Drilling Project
542 (CCSD-PP2) and its geological implication. Acta Petrologica Sinica 23, 3207-3214. (in Chinese with
543 English abstract).
544 Pervozhikov, B. V., Alimov, V. Yu., Tsaritsin, Ye. P., Chashchukhin, I. S., Sherstobitova, L. A., 1990.
545 Chrome spinels and chromite ore deposits of the massif: In: Structure, Evolution and Minerogenesis

546 of the Ray-Iz Ultramafic Massif. The Ural Branch of the Academy of Sciences of the USSR,
547 Sverdlovsk, Russia, p. 149-194 (in Russian)
548 Robinson, P. T., Bai, W.-J., Malpas, J., Yang, J.-S., Zhou, M.-F., Fang, Q.-S., Hu, X.-F., Cameron, S.,
549 Staudigel., H., 2004. Ultra-high pressure minerals in the Luobusa ophiolite, Tibet, and their tectonic
550 implications: Geological Society London, Special Publication 226, 247-271.
551 Rohrbach, A., Ballhaus, C., Golla-Schindler, U., Ulmer, P., Kamenetsky, V.S., Kuzmin, D.V., 2007.
552 Metal saturation in the upper mantle. Nature 449, 456-458.
553 Rollinson, H. R., 2007. Early Earth Systems: a Geochemical Approach. Blackwell Publishing, Oxford,
554 285 pp.
555 Rollinson, H. R., 2008. The geochemistry of mantle chromitites from the northern part of the Oman
556 ophiolite – inferred parental melt compositions: Contributions to Mineralogy and Petrology 156, 273-
557 288.
558 Sameshima, T., Rodgers, K. A., 1990. Crystallography of 6H silicon carbide from Seddonville, New
559 Zealand. Neues Jahrbuch für Mineralogie Monatshefte, 3, 137-143.
560 Savel`ev, A.A., Savel´yeva, G. N., 1977. Ophiolites of the Voykar-Syn´insk massif (Polar Urals).
561 Geotectonics 11, 427-437
562 Savel´yeva, G. N., Suslov, P. V., Larionov, A. N., 2007. Vendian tectono-magmatic events in mantle
563 ophiolitic complexes of the Polar Urals: U-Pb dating of zircon from chromitite. Geotectonics 41, 105-
564 113.
565 Searle, M., Cox, J., 1999. Tectonic setting, origin, and obduction of the Oman Ophiolite: Geological
566 Society of America Bulletin 111, 104-122.
567 Shi, R.-D., Alard, Ol., Zhi, X.-D., O'Reilly, S.Y., Pearson, N. J., Griffin, W. L., Zhang, M., Chen, X -M.,
568 2007. Multiple events in the Neo-Tethyan oceanic upper mantle: Evidence from Ru-Os-Ir alloys in
569 the Luobusa and Dongqiao ophiolitic podiform chromitites, Tibet. Earth and Planetary Science Letters
570 261, 33-48.

571 Shiryaev, A. A., Griffin, W. L., Stoyanov, E., Kagi, H., 2008a. Natural silicon carbide from different
572 geological settings: polytypes, trace elements, inclusions. 9th International Kimberlite Conference,
573 Frankfurt, Extended Abstract 91KC-A-00075.
574 Shiryaev, A. A., Wiedenbeck, M., Polyakov, V. B., Mel´nik, N. N., Lebedev, A. A., Yakimova, R., 2008b.
575 Isotopic heterogeneity in synthetic and natural silicon carbide. Journal of Physics and Chemistry of
576 Solids 69, 2492-2498.
577 Sleep, N. H., Meibom, A., Fridikssonm, T., Coleman, R.G., Bird, D.K., 2004. H_2-rich fluids from
578 serpentinization: geochemical and biotic implications. Proceedings of the National Academy of
579 Sciences of the USA 101, 12818–12823.
580 Soma, T., Matsuo, H., 1982. Pressure derivatives of the melting point for Si and Ge. Journal of Physics C:
581 Solid State Physics 15, 1873-1882.
582 Stachel, T., Brey, G. P., Harris, J. W., 2005. Inclusions in sublithospheric diamonds. Elements 1, 73-78.
583 Svisero, D. P., 1995. Distribution and origin of diamonds in Brazil: An overview. Journal of Geodynamics
584 20, 493-514.
585 Thomassot, E., Cartigny, P., Harris, J. W., Viljoen, K. S., 2007. Methane-related diamond crystallization
586 in the Earth's mantle: stable isotope evidences from a single diamond-bearing xenolith. Earth and
587 Planetary Science Letters 257, 362-371.
588 Ulmer, G. C., Grandstaff, D. E., Woermann, E., Göbbels, M., Schönitz, M., Woodland, A. B., 1998. The
589 redox stability of moissanite (SiC) compared with metal-metal oxide buffers at 1773K and at
590 pressures up to 90 kbar. Neues Jahrbuch Mineralogie Abhandlungen 172, 279-307.
591 Ulmer, G. C., Woermann, E., 2008. Thermodynamic price tags for a wet mantle. Geophysical Research
592 Abstracts, 10, EGU2008-A-12052.
593 Wagner, M. E., Rothman, B., Gleason, J. D., Friedman, J., Carroll, P., Christian, S., 1988. Moissanite
594 (SiC); graphite lens in the Bringhurt Gabbro, northern Delaware. EOS Transactions, American
595 Geophysical Unioin 69, 1483.

596 Xu, S.-T., Wu, W.-P., Xiao, W.-S., Yang, J.-S., Chen, J., Ji, S.-Y., Liu, Y.-C., 2008. Moissanite in
597 serpentinite from the Dabie Mountains in China. Mineralogical Magazine 72, 899-908.
598 Yamamoto, H., Yamamoto, S., Kaneko, Y., Terabasaschi, M., Komiya, T., Katayama, I., Iizuka, T., 2007.
599 Imbricate structure of the Luobusa Ophiolite and surrounding rock units, southern Tibet. Journal of
600 Asian Earth Sciences 29, 296-304
601 Yamamoto, S., Komiya, T., Hirose, K., Maruyama, S., 2009. Coesite and clinopyroxene exsolution
602 lamellae in chromitites: In-situ ultrahigh-pressure evidence from podiform chromitites in the Luobusa
603 ophiolite, southern Tibet. Lithos doi:10.1016/j.lithos.2008.05.003z
604 Yang, J.-S., Dobrzhinetskaya, L., Bai, W.-J., Fang, Q.-S., Robinson, P. T., Zhang, J.-F., Green, H. W. II,
605 2007a. Diamond- and coesite-bearing chromitites from the Luobusa ophiolite, Tibet. Geology 35, 875-
606 878.
607 Yang, J.-S., Bai, W.-J., Fang, Q.-S., Meng, F.-C., Chen, S.-Y., Zhang, Z.-M., 2007b, Diamond and
608 unusual minerals discovered from the chromitite in Polar Ural: A first report. Eos Transactions,
609 American Geophysical Union, Fall Meeting Supplement. V43E-05.
610 Zhang, Z., Mao, J., Wang, F., Pirajno, F., 2006. Native gold and native copper grains enclosed by olivine
611 phenocrysts in a picrite lava of the Emeishan large igneous province, SW China. American
612 Mineralogist 91, 1178-1183.
613 Zhou, M.-F., Malpas, J., Robinson, P. T., Reynolds, P., 1997. The dynamothermal aureole of the
614 Dongqiao ophiolite, northern Tibet. Canadian Journal of Earth Science 34, 59-65.
615 Zhou, M.-F., Robinson, P. T., Malpas, J., Li Z.-T., 1996. Podiform chromites in the Luobusa ophiolite
616 (Southern Tibet): implications for melt-rock interaction and chromite segregation in the upper mantle:
617 Journal of Petrology 37, 3-21.
618 Zhou, M.-F., Robinson, P. T., Malpas, J., Edwards, S. J., Qi, L., 2005. REE and PGE geochemical
619 constraints on the formation of dunites in the Luobusa Ophiolite, southern Tibet. Journal of Petrology
620 46, 615-639.
621

622

623 **Figure captions**

624

625 Figure 1. Location map of the ophiolites sampled from this study; 1: Luobusa, 2: Dongqiao, 3: Semail, 4:
626 Ray-Iz.

627 Figure 2. Photomicrographs of moissanite from ophiolites. (a) loose moissanite grains from Luobusa
628 orebody 31 (PPL). Note the euhedral outline of several grains, the round to ovoid inclusions of Si
629 (circled) and optical zoning in one grain (lower center). The dark grains at the top of the image are
630 graphite; (b) moissanite grain from the Semail ophiolite (PPL) with small ovoid inclusion of Si
631 (circled); (c) angular moissanite fragments from Ray-Iz ophiolite with large, rounded Si inclusions
632 (reflected light); (d) back-scattered electron image of the inclusion in (b) showing grains of Fe-Si
633 alloy at the margin of the Si inclusion in moissanite.

634 Figure 3. Frequency histograms showing the C-isotope composition of moissanites from ophiolites
635 determined in this study (upper panels separately for each locality) and a stacked histogram (lower
636 panel) with all moissanite $\delta^{13}C$ values compiled from our study and the literature. Key for references
637 to moissanite data: (1) this study; plus two analyses from Armenia in Marshintsev, (1990), (2) Di
638 Pierro et al., 2003; (3) Mathez et al., 1995; (4) Marschintsev, 1990; (5) Leung et al., 1990; (6) Wagner
639 et al. 1988. Also shown in gray shading on the lower panel is the relative frequency distribution of
640 $\delta^{13}C$ values from 997 eclogite-type diamonds (modified from Cartigny, 2005).

641

642

643 **Appendix**

644

645 The carbon isotope ratio of synthetic SiC reference material used for SIMS analyses was measured after
646 sample combustion in a Carlo Erba EA-1500 reactor connected to a ThermoFisher Delta V Plus mass
647 spectrometer. The sample was individually wrapped in tin foil cups and dropped into the reactor with a
648 small dose of oxygen gas mixed into the He stream. The sample was then oxidized in the reactor held at
649 1050°C and filled with cobaltous oxide as a catalyst for the oxidation. Excess oxygen from the He-stream
650 was adsorbed in another reactor column filled with metallic Cu held at 500°C. The residual gases of CO_2,
651 (N_2), and H_2O were then passed over a water trap of magnesium perchlorate ($Mg(ClO_4)_2$) and into a gas
652 chromatograph filled with a molecular sieve (5A) to separate N_2 and CO_2. The CO_2 was transported by the
653 He-stream via a CONFLO III (open split) system into the mass spectrometer for isotopic analyses. The
654 sample yields using this procedure were between 90 and 100%. Reproducibility of the internal graphite
655 standard used was better than 0.10‰ and USGS-24 graphite (–16.0 per mil VPDB) and NBS-22 oil (-29.6
656 per mil VPDB) were used as calibration standards. The results for duplicate analyses of the reference SiC
657 GFZ-S113 are $\delta^{13}C$ values of –28.71 and –28.79‰.

658

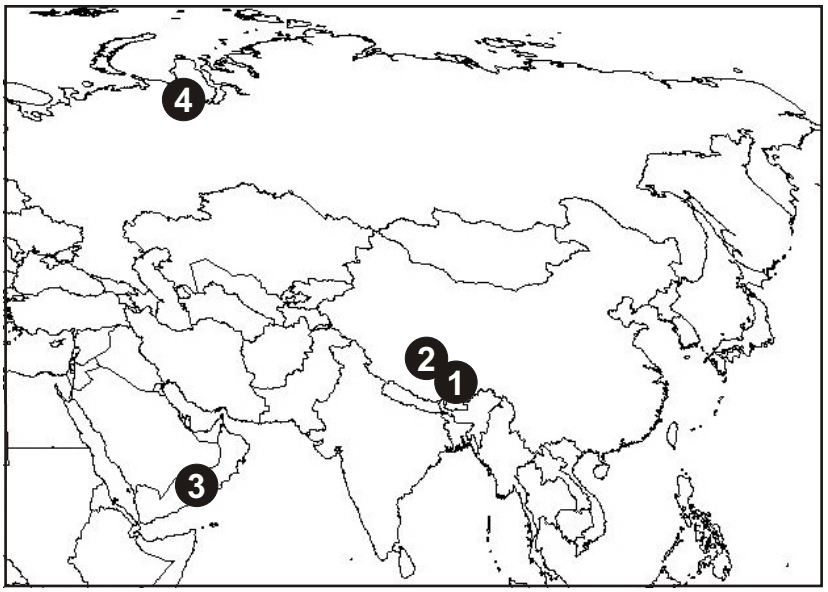

Figure 1

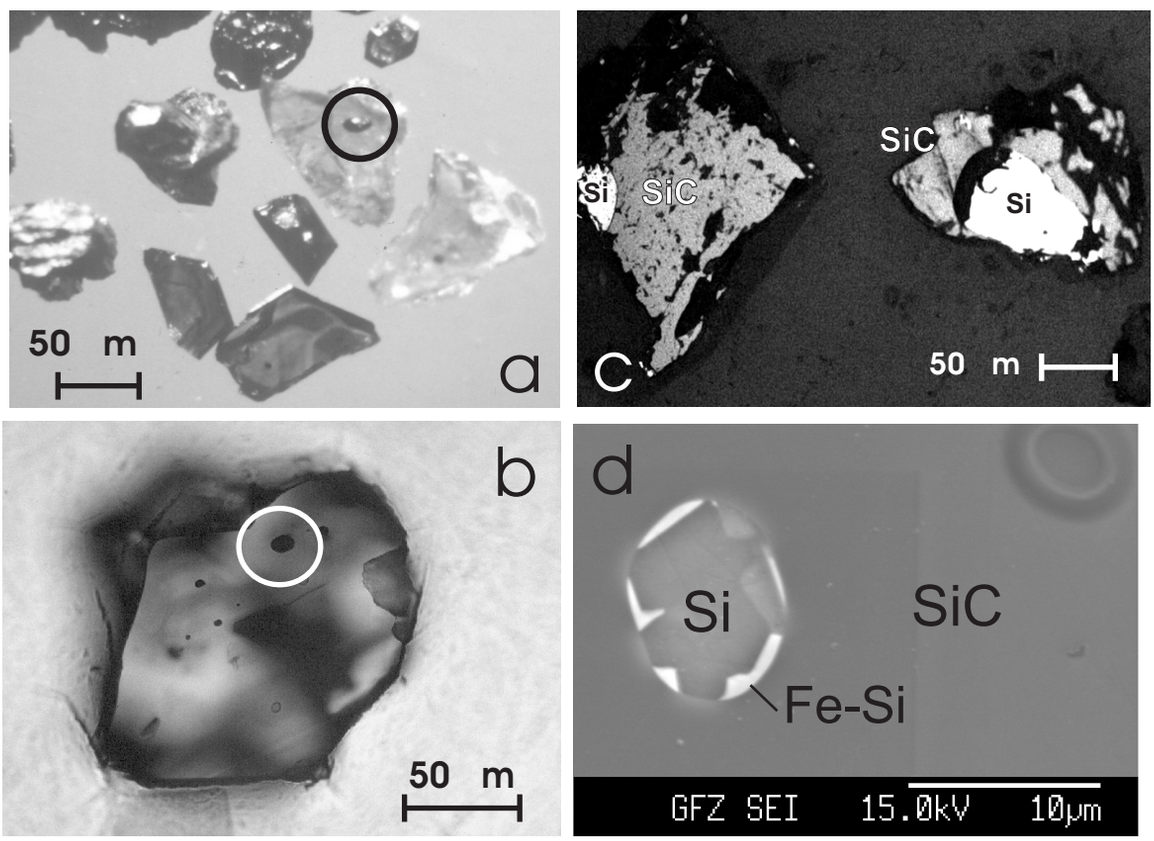

Figure 2

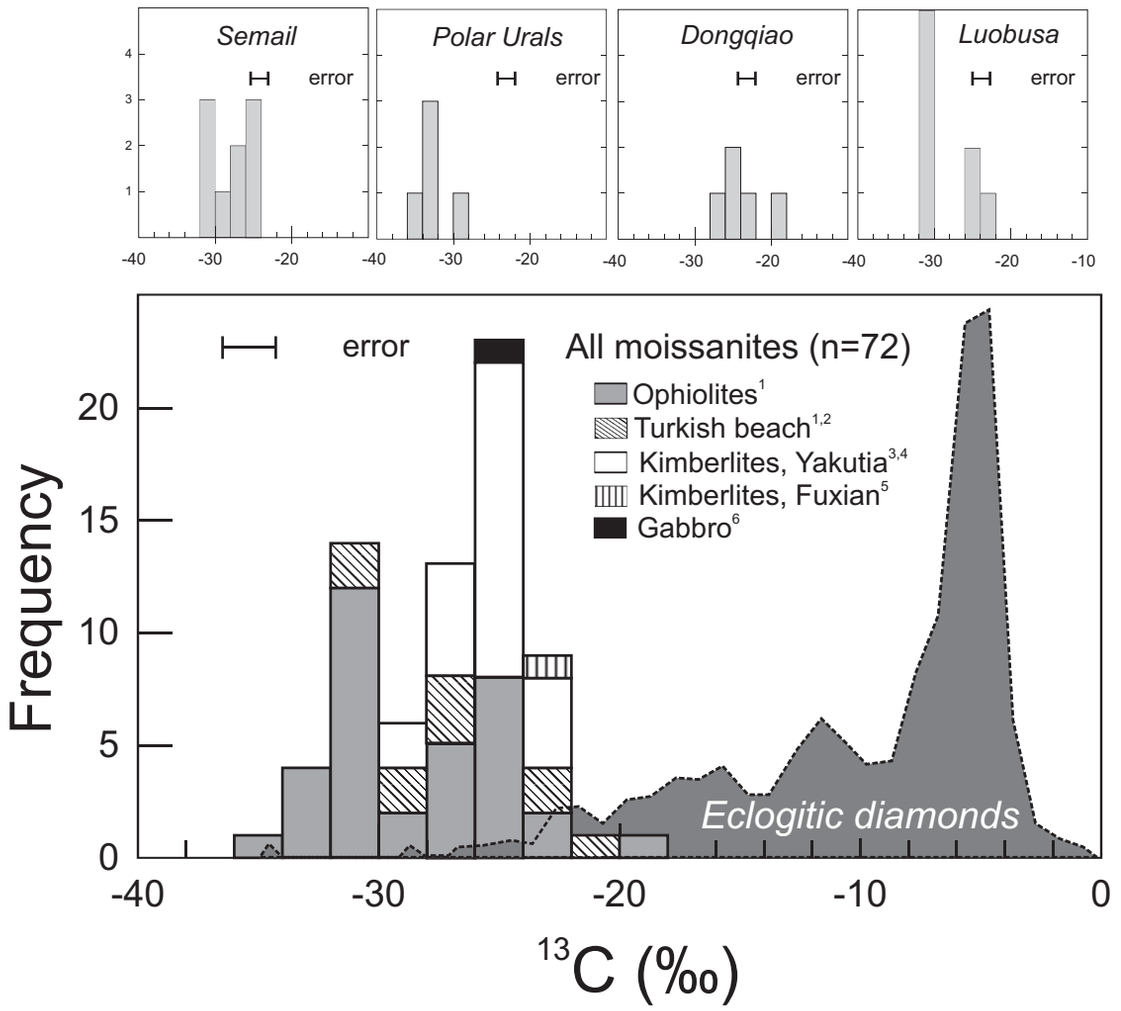
Semail
Polar Urals
Dongqiao
Luobusa
error
All moissanites (n=72)
Ophiolites[1]
Turkish beach[1,2]
Kimberlites, Yakutia[3,4]
Kimberlites, Fuxian[5]
Gabbro[6]
Eclogitic diamonds
Frequency
^{13}C (‰)

Figure 3

Table 1

Click here to download Table: Table 1.xls

Table 1. Results of SIMS measurements on SiC reference materials

Analysis	Sample	Grain	$^{13}C/^{12}C$ (meas.)	precision[a]	IMF[b]	$\delta^{13}C$[c]
GFZ-S113 ($^{13}C/^{12}C$ = 0.109141 and $\delta^{13}C$ = -28.75)						
PRmar009	S113	G1	0.01059	1.14	0.0970	-26.5
PRmar013	S113	G1	0.01056	1.08	0.0968	-29.2
PRmar014	S113	G1	0.01059	0.98	0.0970	-26.5
PRmar015	S113	G1	0.01060	1.11	0.0971	-25.5
PRmar021	S113	G1	0.01060	1.10	0.0971	-25.5
PRmar023	S113	G2	0.01057	1.17	0.0968	-28.3
PRmar028	S113	G1	0.01055	1.05	0.0967	-30.1
PRmar036	S113	G1	0.01057	1.04	0.0968	-28.3
PRmar037	S113	G1	0.01054	0.94	0.0966	-31.0
PRmar038	S113	G2	0.01055	1.34	0.0967	-30.1
PRmar042	S113	G2	0.01057	1.15	0.0968	-28.3
PRmar048	S113	G1	0.01054	1.06	0.0966	-31.0
PRMar049	S113	G1	0.01057	0.98	0.0968	-28.3
PRmar060	S113	G1	0.01055	1.16	0.0967	-30.1
PRmar063	S113	G1	0.01055	1.07	0.0967	-30.1
PRmar064	S113	G1	0.01056	1.02	0.0968	-29.2
PRmar070	S113	G2	0.01053	1.21	0.0965	-32.0
PRmar075	S113	G1	0.01058	1.04	0.0969	-27.4
Mean			0.01057			-28.8
Repeatability in permil [d]			1.98			
AMNH-100578 ($^{13}C/^{12}C$ = 0.109441 and $\delta^{13}C$ = -26.1)						
PRmar047	AMNH 100578	G1	0.01061	1.10	0.0969	-24.6
PRmar057	AMNH 100578	G2	0.01061	0.96	0.0969	-24.6
PRmar058	AMNH 100578	G3	0.01058	1.06	0.0967	-27.4
PRmar059	AMNH 100578	G4	0.01061	1.14	0.0969	-24.6
PRmar065	AMNH 100578	G5	0.01059	1.11	0.0968	-26.5
PRmar066	AMNH 100578	G6	0.01061	1.01	0.0969	-24.6
Mean			0.01060			-25.4
External precision in permil [d]			1.25			

Values for S113 from this study (see text), for AMNH 100578 from Mathez et al. (1995)

a) Analytical uncertainty in permil (1 σ) for each analysis of 80 cycles

b) Instrumental mass fractionation ($^{13}C/^{12}C$measured / $^{13}C/^{12}C$ reference material)

c) values in permil relative to the zero-value reference PDB ($^{13}C/^{12}C$ = 0.112372)

d) Repeatability based on multiple analyses of reference SiC (1σ / mean)*1000

Table 2

Click here to download Table: Table 2new.xls

Table 2. Results of in-situ C-isotope composition of moissanites by SIMS

Locality	Sample-Grain	$^{13}C/^{12}C$ (meas.)	precision[a]	$^{13}C/^{12}C$ (corr.)[b]	$\delta^{13}C$[c]
Rai-iz ophiolite	J-2	0.01052	0.115	0.10868	-32.9
Rai-iz ophiolite	J-4	0.01051	0.114	0.10857	-33.8
Rai-iz ophiolite	K-1	0.01052	0.117	0.10868	-32.9
Rai-iz ophiolite	K-6	0.01050	0.098	0.10847	-34.7
Rai-iz ophiolite	K11	0.01056	0.103	0.10909	-29.2
Luobusa ophiolite	F-1	0.01054	0.105	0.10888	-31.0
Luobusa ophiolite	F-2	0.01054	0.119	0.10888	-31.0
Luobusa ophiolite	F-4	0.01060	0.126	0.10950	-25.5
Luobusa ophiolite	F-7	0.01054	0.118	0.10888	-31.0
Luobusa ophiolite	G1	0.01063	0.125	0.10981	-22.8
Luobusa ophiolite	G1b	0.01060	0.116	0.10950	-25.5
Luobusa ophiolite	G2	0.01055	0.102	0.10899	-30.1
Luobusa ophiolite	G3	0.01055	0.109	0.10899	-30.1
Dongqiao ophiolite	G1	0.01058	0.105	0.10930	-27.4
Dongqiao ophiolite	G2	0.01061	0.119	0.10961	-24.6
Dongqiao ophiolite	G2	0.01068	0.133	0.11033	-18.2
Dongqiao ophiolite	G3	0.01061	0.109	0.10961	-24.6
Dongqiao ophiolite	G4	0.01063	0.105	0.10981	-22.8
Semail ophiolite	UAE1-1	0.01055	0.105	0.10899	-30.1
Semail ophiolite	UAE1-2	0.01053	0.102	0.10878	-32.0
Semail ophiolite	UAE1-2b	0.01056	0.105	0.10909	-29.2
Semail ophiolite	UAE1-3	0.01060	0.095	0.10950	-25.5
Semail ophiolite	OM2-G1	0.01054	0.094	0.10888	-31.0
Semail ophiolite	OM2-G2	0.01059	0.107	0.10940	-26.5
Semail ophiolite	OM2-G3	0.01058	0.110	0.10930	-27.4
Semail ophiolite	OM2-G4	0.01060	0.107	0.10950	-25.5
Semail ophiolite	OM2-G5	0.01060	0.113	0.10950	-25.5
Turkish beach**	G1	0.01062	0.113	0.10971	-23.7
Turkish beach	G1b	0.01054	0.098	0.10888	-31.0
Turkish beach	G2	0.01058	0.105	0.10930	-27.4
Turkish beach	G2b	0.01057	0.107	0.10919	-28.3
Turkish beach	G3	0.01057	0.102	0.10919	-28.3
Turkish beach	G3b	0.01065	0.124	0.11002	-20.9
Turkish beach	G3c	0.01055	0.100	0.10899	-30.1
Turkish beach	G4	0.01063	0.148	0.10981	-22.8
Turkish beach	G5	0.01058	0.119	0.10930	-27.4

Ophiolite samples are podiform chromitites except for Luobusa F-1, F-2, F-4 which are peridotite hostrock

a - Analytical uncertainty in permil (1 σ) for each analysis of 80 cycles

b - ratio corrected for instrumental mass fractionation based on SiC reference materials (Table 1)

c- values in permil relative to the zero-value reference PDB ($^{13}C/^{12}C$ = 0.112372)

** Moissanite-rich ultramafic volcanic sample found on Turkish beach (di Pierro et al., 2003)